Biophysical Chemistry 29 (1988) 327–339
Elsevier

BPC 01244

An analysis of the hyper-sharp phenomenon of myosin diffusion in an F-actin / ATP solution by computer simulation

Hiroshi Kagawa [a], Yoshinori Nagai [b] and Hiroshi Asai [c]

[a] *Department of Physics, Nippon Ika University, Kawasaki, Kanagawa 211,*
[b] *Laboratory of Molecular Biology, School of Veterinary Medicine, Azabu University, Sagamihara, Kanagawa 229 and* [c] *Department of Physics, School of Science and Engineering, Waseda University, Shinjuku, Tokyo 160, Japan*

Received 4 June 1987
Revised manuscript received 19 November 1987
Accepted 7 December 1987

Muscle contraction; Myosin; Active diffusion; Hyper-sharp phenomenon; Computer simulation; Random walk

The diffusion of myosin molecules was demonstrated using schlieren optics and Rayleigh fringe optics. A hyper-sharp schlieren pattern appeared near the boundary between the upper and lower parts of the diffusion cell at a time when ATP in the lower part had almost been consumed. The mechanism underlying the appearance of the hyper-sharp peak was investigated by means of computer simulations based on random-walk theory. The schlieren pattern with the hyper-sharp peak could be reproduced on the computer with the assumptions that a myosin molecule can be detached from an actin filament only on binding of ATP and that it can then move along actin filaments or diffuse in the aqueous solution. The results of the computer simulations are in good agreement with the experimental data.

1. Introduction

The sliding theory of muscular contraction is widely accepted. However, in spite of much effort, the details of the sliding mechanism at the molecular level have not yet been elucidated. One of the authors of the present article (H.A.) has proposed a method for the detection of in vitro sliding as 'active diffusion' [1] of myosin molecules on actin filaments. Therefore, in a previous study [2], we measured the translational diffusion coefficients for molecules of myosin in a solution of F-actin and ATP and carried out computer simulations based on calculus of finite differences to detect active diffusion by comparing experimental results with simulated curves, the hyper-sharp peak being ignored. We found from the simulations that the schlieren pattern at low ATP concentration is not Gaussian but asymmetrical. We also determined the diffusion coefficient for heavy meromyosin (HMM) in F-actin/ATP solution under conditions where actin-activated ATPase activity is close to its maximal value at a very low electrolyte concentration (the fraction of HMM bound to actin, f, being relatively high), and have obtained results which support the idea that HMM slides actively along actin filaments in solution [3]. In experiments aimed at detecting active diffusion, we observed the so-called hyper-sharp phenomenon, which was seen when ATP in the lower part of the diffusion cell had almost been consumed [4].

To ascertain the origin of this phenomenon and to determine whether active diffusion is involved in the appearance of the hyper-sharp peak, we attempted computer simulations with the assumptions that a myosin molecule becomes detached

Correspondence address: H. Kagawa, Department of Physics, Nippon Ika University, 2-297-2 Kosugi, Kawasaki, Kanagawa 211, Japan.

0301-4622/88/$03.50 © 1988 Elsevier Science Publishers B.V. (Biomedical Division)

from an actin filament and diffuses actively or freely only on binding to an ATP molecule. In this paper, in contrast with the previous article [2], we performed the simulations under conditions where the hyper-sharp phenomenon occurs. The simulation results are in good agreement with our experimental data.

In section 2 we summarize the experimental data for comparison with the results obtained from computer simulations.

The model used in computer simulations is described in section 3. In computer simulation we varied the parameters over wide ranges, some of which could not be realized in actual experiments. In simulations random walks [5] were chosen to model the movement of molecules. The transition probabilities of walkers were determined from diffusion coefficients. The relation between these quantities is derived in the appendix.

In section 4 we discuss the origin of the hyper-sharp phenomenon and the possibility of detecting active diffusion by analyzing this event.

2. Summary of diffusion experiments

Here, we summarize our experimental results concerning the hyper-sharp phenomenon and active diffusion. In the experiments we observed diffusion of myosin (myosin A, HMM or myosin subfragment-1 (S-1)) in F-actin/ATP solutions. The upper part of a Neurath-type diffusion cell [6] was filled with F-actin and ATP, the lower part with F-actin, ATP and myosin, both parts then being brought into contact so that a boundary between the two solutions was formed and diffusion of myosin in F-actin/ATP solutions began. Diffusion patterns were observed as concentration gradient distributions of myosin molecules with schlieren optics [4] or as concentration distribu-

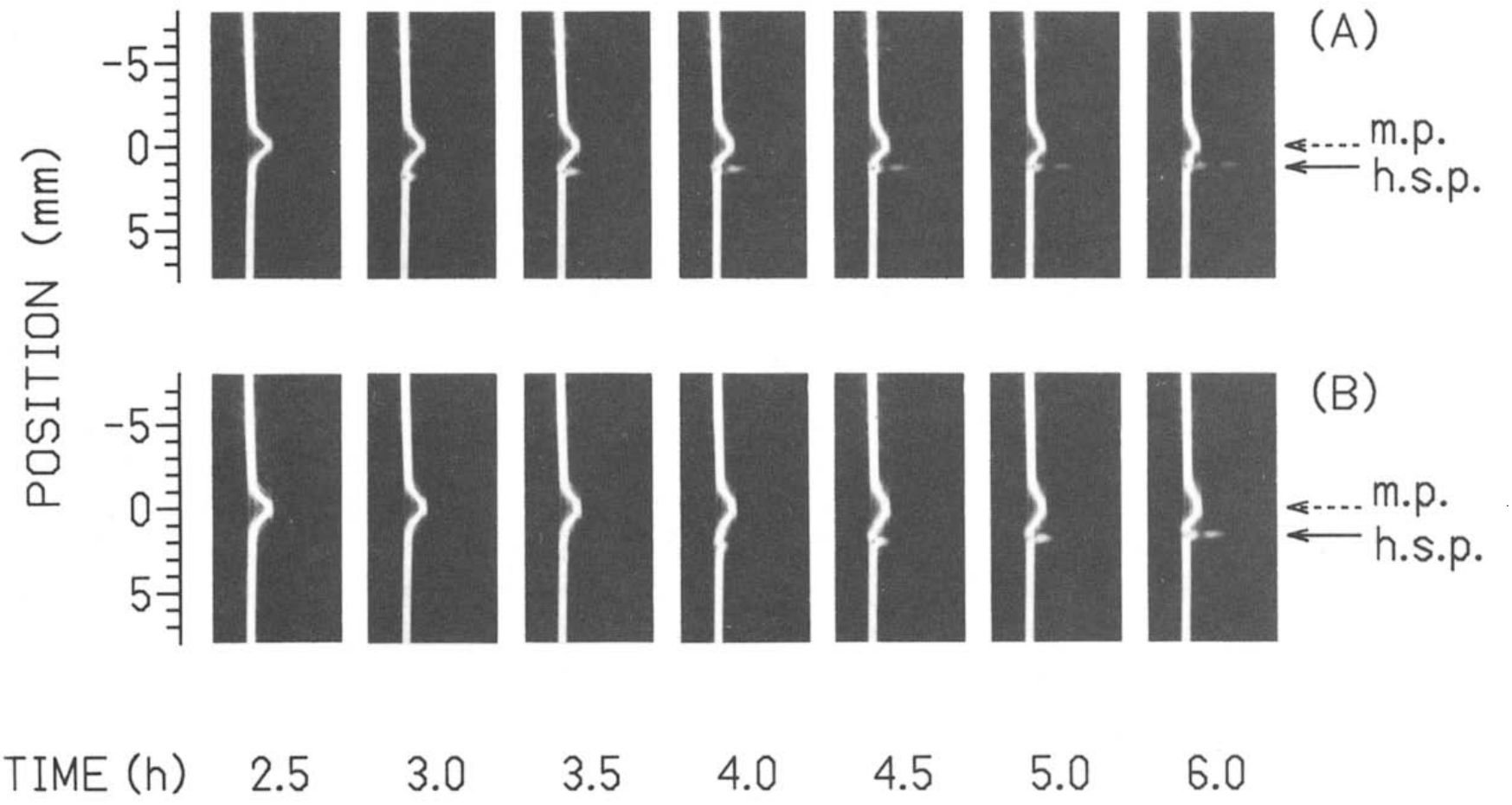

Fig. 1. Typical schlieren patterns with a hyper-sharp peak. Arrows marked h.s.p. and m.p. indicate the hyper-sharp peaks and main peaks, respectively. The units for position correspond to the real measure of the diffusion cell. The value of the position indicates the distance from the synthetic boundary in the cell (+, downward; −, upward). Photographs were obtained with schlieren optics on a Hitachi HTD-1 Tiselius-type electrophoretic apparatus. Prints were reproduced from slightly overexposed negatives in which hyper-sharp peaks are relatively clear although other parts of the patterns are not sharp, noise being evident. Solution conditions: 1.53 mg/ml HMM, 0.65 mg/ml F-actin with native tropomyosin, 10 mM MgATP, 0.1 M KCl, 0.1 mM $CaCl_2$ (A) or 1 mM EGTA (B), 10 mM Tris-maleate, pH 6.8, 25.0 °C. Bar angle: 30 °.

tions with Rayleigh fringe optics. In the schlieren pattern the hyper-sharp peak appeared near the boundary when almost all ATP in the lower part of the cell had been consumed. With Rayleigh fringe optics this phenomenon was observed as a steep cliff with small bumps in the concentration distribution curves.

Typical patterns are shown in figs. 1 and 2. Fig. 1 demonstrates the diffusion schlieren patterns of HMM in F-actin (decorated with native tropomyosin)/ATP solution in the presence (A) or absence (B) of Ca^{2+} at various times. 3 h (fig. 1A) and 4 h (fig. 1B) after diffusion had begun a small sharp peak appeared in the lower part of the diffusion cell. This peak became more distinct and its height increased; we therefore designated this as the hyper-sharp peak. On the other hand, the Gaussian main peak decreased in height and broadened as diffusion proceeded.

Based on the photographs of fig. 1, the time course for the change in height and position of the hyper-sharp peak is plotted in figs. 3 and 4, respectively. As shown in fig. 4, the hyper-sharp peak appears at a lower position than the main peak, and moves rapidly upward initially, its movement then becoming increasingly slower.

As mentioned in a previous paper [4], after the F-actin/ATP/HMM solution had been injected into the lower part of the cell, an aliquot of the same solution remaining in a test tube was used concurrently to estimate the concentration of unhydrolyzed ATP by measuring the level of P_i liberated. According to this measurement, it was found that at the moment when the small sharp peak began to appear, almost all ATP in the lower part of the cell had been consumed. Therefore, it is clear that the difference in the moment of onset of the peak between panels A and B in fig. 1 is due to the difference in rate constants for ATP hydrolysis under these conditions. After the hyper-sharp peak had appeared, in the upper part of the cell to which HMM had not yet diffused, ATP was not yet consumed. Therefore, ATP still diffused into the lower part of the cell, so that the features of both the hyper-sharp and main peaks changed gradually even after the appearance of the hyper-sharp peak.

As reported in our previous article [4], the hyper-sharp phenomenon was observed in 0, 0.05, 0.1, 0.6 and 0.75 M KCl and in the presence of

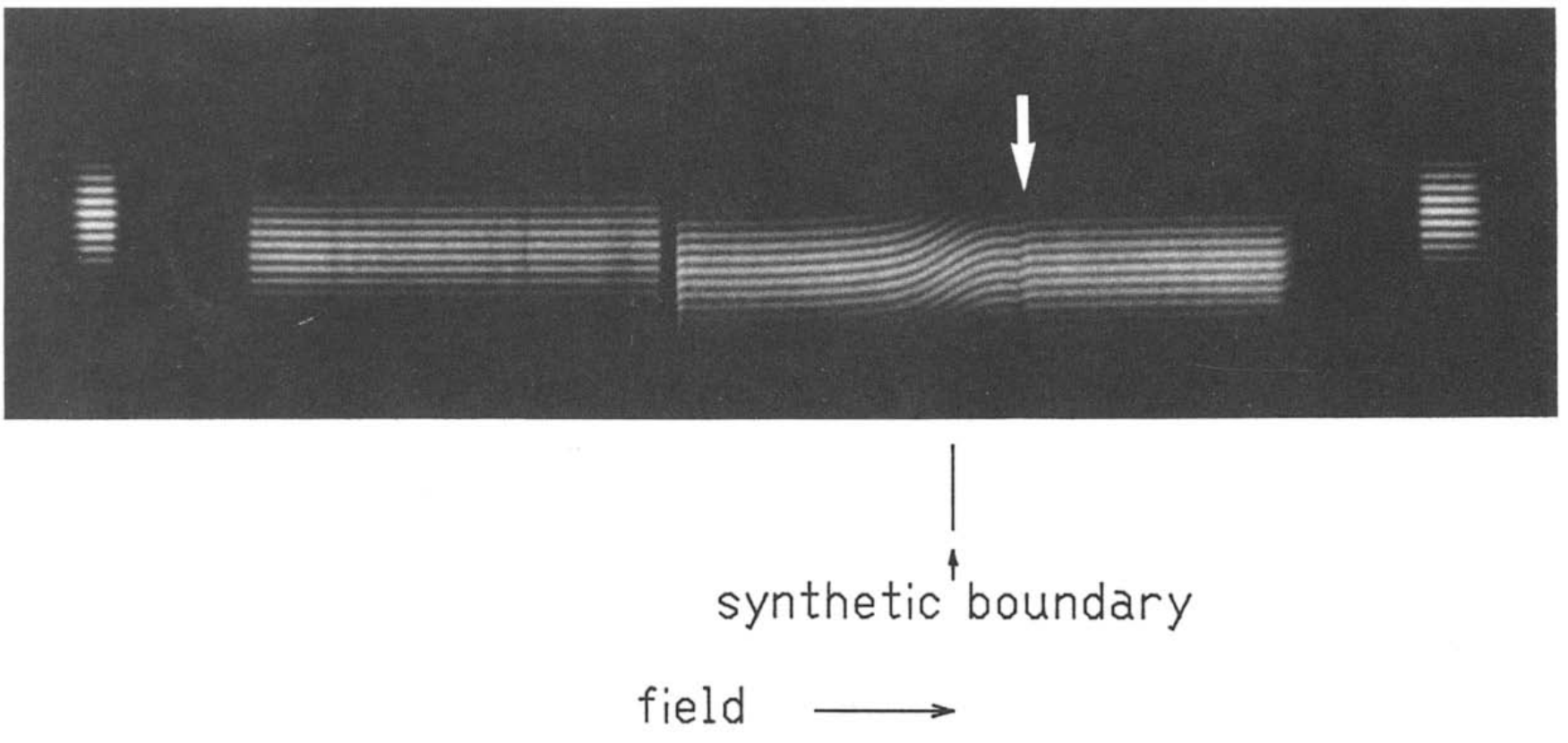

Fig. 2. Typical pattern of concentration distribution with the hyper-sharp phenomenon. Downward arrow indicates a steep cliff corresponding to the hyper-sharp peak in the schlieren pattern. Photograph obtained with Rayleigh fringe optics on a Hitachi 282 analytical ultracentrifuge (at 650 × g). Solution conditions: 1 mg/ml HMM, 1 mg/ml F-actin, 5 mM MgATP, 50 mM KCl, 10 mM Tris, pH 7.95, 27.5 ° C. Time after diffusion commenced: 30 min.

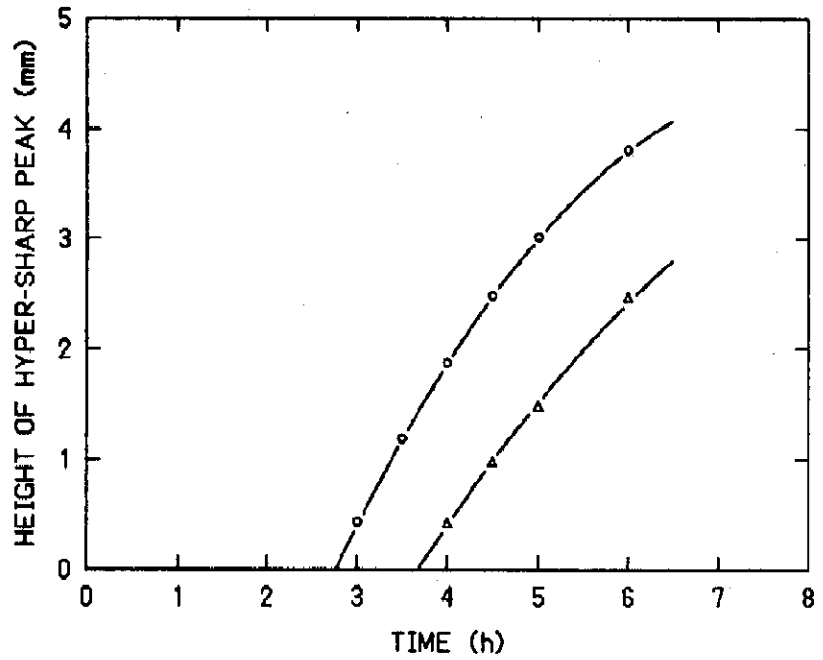

Fig. 3. Experimental time course of change in height of hyper-sharp peak. Values of the height were directly measured on the negatives for fig. 1 with a Mitutoyo PV-350 comparator. $+Ca^{2+}$ (○ (A)), $-Ca^{2+}$ (△ (B)).

Mg^{2+} or Ca^{2+}. On the other hand, the hyper-sharp phenomenon and diffusion of HMM were barely detectable in the presence of 1 mM EDTA and 0.1 M KCl, since, under these conditions, HMM dissociates from F-actin to only a very small degree. Accordingly, the hyper-sharp peak appeared in the case where both actin filaments and ATP molecules were present in the solution and myosin molecules could become detached from F-actin by binding ATP.

The hyper-sharp phenomenon occurred not only with HMM but also with soluble myosin A (in KCl at above 0.3 M) or S-1.

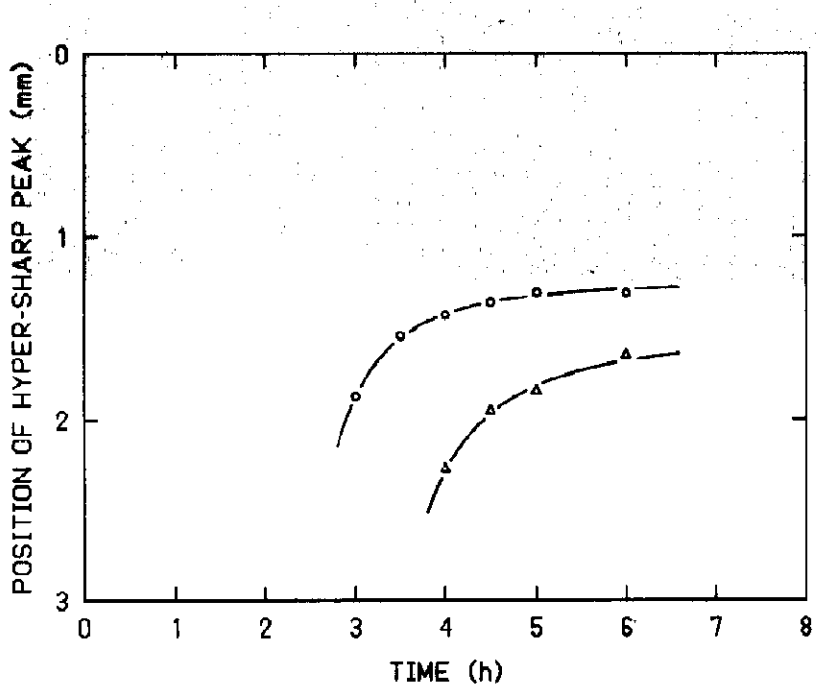

Fig. 4. Experimental time course of change in position of hyper-sharp peak. Values of position obtained as in fig. 3. $+Ca^{2+}$ (○ (A)), $-Ca^{2+}$ (△ (B)).

A typical example of the hyper-sharp phenomenon was observed at concentrations greater than 0.2 mg/ml of myosin A, HMM or S-1, when the molar ratio to actin was varied from 1 : 1 to 1 : 12. The value of 0.2 mg/ml is only the lower limit for clear observation of the hyper-sharp peak with schlieren optics on a Hitachi HTD-1 Tiselius electrophoretic apparatus. Even below 0.2 mg/ml of myosin, the hyper-sharp peak could be observed. Because of its sharpness the hyper-sharp peak was usually faint on photographs, as in fig. 1, but was very clear to the naked eye. The reproducibility of this phenomenon was almost 100%.

The schlieren patterns obtained from our diffusion experiments with the hyper-sharp and main peaks closely resemble those from the sedimentation experiments of Joseph and Harrington (fig. 1a and b in ref. 7). Their schlieren patterns also exhibit both a hyper-sharp and a broad peak. However, our phenomenon should originate from an entirely different effect, for the following reasons:

(1) Our hyper-sharp phenomenon did not occur in the absence of F-actin, whereas the experiments of Joseph and Harrington were performed without actin.

(2) Our hyper-sharp phenomenon occurred without acceleration for sedimentation (at $1 \times g$ in a Neurath-type diffusion cell or $650 \times g$ in that of an analytical ultracentrifuge, only for avoiding tilting of the solution due to gravity), whereas theirs took place for the centrifugal field routinely used for sedimentation.

(3) Our hyper-sharp peak rose upward (or in the centripetal direction), whereas theirs should move centrifugally.

In the previous study [4], we examined three possible molecular mechanisms of the hyper-sharp phenomenon. The first possibility is the overall or local contraction of a gel composed of myosin (or its proteolytic fragments) and F-actin which might give rise to a steep cliff in the concentration distribution of proteins. However, it is very difficult to explain the upward movement of the hyper-sharp peak by invoking a mechanism of gel contraction. Moreover, the hyper-sharp phenome-

Table 1

Diffusion coefficients of HMM and myosin A

Conditions for experiments with HMM: 1 mg/ml HMM, 3 mM ATP, 3 mM $MgCl_2$, 3 mM imidazole, 2.7 mM P_i, 0.1 mM EGTA, pH 7.0 [4]. Conditions for myosin A: 1.3 mg/ml myosin A, 1 mM ATP, 2 mM $MgCl_2$, 20 mM Tris-maleate, pH 7.0.

	[Actin] (mg/ml)	Diffusion coefficient ($cm^2\ s^{-1}$) ($\times 10^{-7}$)		
		0.5 °C, no KCl	0.5 °C, 0.1 M KCl	25.0 °C, 0.3 M KCl
HMM	0	1.08–1.14	1.20–1.24	
	0.5	1.11–1.17	1.19–1.25	
	1.0	1.11–1.18	1.18–1.25	
Myosin A	0			1.3
	0.26			1.3

non also occurred with S-1 as mentioned above, and since S-1 cannot cross-bridge two actin filaments and thus is unable to form a gel with F-actin, this possibility was not considered to be the correct explanation for the hyper-sharp phenomenon. In addition, some experimental data are in support of this conclusion [4].

The second mechanism involves the local accumulation of myosin molecules on actin filaments just beneath the hyper-sharp peak, whose position coincides with the boundary of the ATP-deficient region. This was considered to be inconsistent with the fact that in experiments with an ATP-regenerating system, the hyper-sharp peak still appeared despite the presence of a small amount of ATP in the lower part of the cell where myosin molecules could not permanently accumulate on actin filaments. However, simulations of this work demonstrate that this possibility is a suitable explanation for this phenomenon.

Finally, active migration or active diffusion of myosin molecules on F-actin filaments provides the third possibility. This had been considered to be the most probable, however, the hyper-sharp phenomenon itself does not represent direct evidence of active migration.

We now discuss briefly experimental data for diffusion coefficients of myosin molecules with respect to active diffusion. In fig. 1, the main peak is indicated by the arrows denoted m.p. By measuring the broadening of the main peak with respect to time, we are able to calculate the diffusion coefficients of materials undergoing diffusion. It is clear from our experimental data (a number of which are listed in table 1) that the diffusion coefficients of myosin molecules in the presence of actin filaments and ATP did not significantly differ from those in the absence of actin filaments. Such results are reasonable in view of the low affinity of soluble myosin or HMM for F-actin in the presence of sufficient ATP.

3. Computer simulation

3.1. Model

To determine at the molecular level how the mechanism of sliding of myosin molecules on actin filaments results in the hyper-sharp phenomenon, we proposed a hypothetical scheme which we then simulated on a computer. Random walks are usually employed in the analysis of diffusion processes. We therefore constructed a model in which diffusing molecules migrate in a series of random walks. Actin filaments in a solution are assumed to be homogeneously and randomly distributed, and thus, at the molecular level, do not cause movement of myosin molecules in a single direction. We assumed that actin filaments are fixed in space, since their diffusion coefficient is much smaller than those of soluble myosin or ATP. We used the simple kinetic scheme expressed by

$$\mathrm{AM} + \mathrm{S} \overset{K}{\rightleftarrows} \mathrm{MS} + \mathrm{A} \overset{k_2}{\rightarrow} \mathrm{AM} + \mathrm{P} \qquad (1)$$

where AM denotes actomyosin, S the substrate (ATP), MS the myosin-substrate complex, P the products ($ADP + P_i$), K the equilibrium constant ([MS][A]/[AM][S]), and k_2 the rate constant of ATP hydrolysis. Interactions between a myosin molecule and an actin filament were assumed to have the following characteristics: (1) A myosin molecule binds to an actin filament and does not move in the absence of ATP. (2) A myosin molecule can become detached from an actin filament

when ATP binds to myosin. (3) A myosin molecule which has become detached from an actin filament slides along the actin filament or diffuses in solution. (4) A myosin molecule, on binding to ATP, catalyzes ATP hydrolysis to ADP and P_i with a certain probability according to the rate constant, k_2.

Essentially, the schlieren and Rayleigh fringe patterns were observed experimentally in a single dimension. Hence, we assumed that every molecule moves in a one-dimensional space. Simulations were performed via a combination of three kinds of processes, namely, migration of molecules (MS and S), hydrolysis of S (i.e., ATP), and recovery of equilibrium. The hydrolysis of S perturbs the equilibrium between AM + S and MS + A, so that a process of recovery of equilibrium is required.

Furthermore, it is conceivable that the process of recovery of equilibrium is necessary not only after hydrolysis but also after migration, since migration of MS and S also results in deviations from equilibrium. Therefore, we carried out simulations for both of the following cases: (1) a single process of recovery of equilibrium after hydrolysis, and (2) two processes after hydrolysis and after migration. The result for the former case was in good agreement with that of the latter. This means that only the process of recovery of equilibrium after hydrolysis is essential for simulation of the hyper-sharp phenomenon. Hence, we analyzed the hyper-sharp phenomenon by means of simulations using the cyclic sequence of processes described above, namely, migration → hydrolysis → recovery of equilibrium.

As stated above, all molecules which are able to diffuse are represented as random walkers. In random-walk theory, knowledge of the transition probabilities is essential for describing the process. Experimentally, however only the diffusion coefficients are measurable. Thus, we require an expression for the relation between the transition probabilities and the diffusion coefficient. The resultant for one-dimensional cases is

$$D = \frac{1}{2}\sum_{j=1}^{k}[p_j + q_j]\, j^2 \frac{(\Delta x)^2}{\Delta t} \qquad (2)$$

where D denotes the diffusion coefficient, p_j (q_j) the transition probability of the walker jumping to the j-th separated site in the positive (negative) direction, Δx the lattice distance and Δt the unit interval of time. Note that in eq. 2 the walker cannot jump beyond the k-th site distant from the occupied site. Details of the derivation of eq. 2 are given in the appendix.

3.2. Methods for simulations

To elucidate the mechanism underlying the hyper-sharp phenomenon, we examined several cases where the parameters of the above model are varied. In our model, passive and active diffusion can be simulated by changing the distribution of transition probabilities. Typical examples of transition probabilities for the passive and active diffusion of myosin are illustrated in fig. 5. The diffusion coefficients used were $D_{\mathrm{MS\ passive}} = 2 \times 10^{-7}$ cm^2 s^{-1} and $D_{\mathrm{ATP}} = 73 \times 10^{-7}$ cm^2 s^{-1}, which were measured at 25.0 °C.

In the simulations we usually used the equilibrium constant $K = 10$ for $\mathrm{AM + S} \rightleftarrows \mathrm{MS + A}$ and the rate constant $k_2 = 0.02\ \mu\mathrm{M}^{-1}\ \mathrm{s}^{-1}$ for $\mathrm{MS + A} \rightarrow \mathrm{AM + P}$. The initial concentration of each species was taken appropriately. For simulations, we used values of $[\mathrm{M_{total}}] = (0\ \mu\mathrm{M}$ for $x = 1$–1000, $3\ \mu\mathrm{M}$ for $x = 1001$–$2000)$, $[\mathrm{A_{total}}] = 24\ \mu\mathrm{M}$ for $x = 1$–2000, and $[\mathrm{S_{total}}] = 5$ mM for $x = 1$–2000 ($[\mathrm{M_{total}}] = [\mathrm{MS}] + [\mathrm{AM}]$, $[\mathrm{A_{total}}] = [\mathrm{A}] + [\mathrm{AM}]$, $[\mathrm{S_{total}}] = [\mathrm{S}] + [\mathrm{MS}]$). In addition, we selected values of $\Delta t = 0.5$ s and $\Delta x = (0.2)^{1/2} \times 10^{-3}$ cm, respectively.

For passive diffusion we employed a Gaussian distribution of transition probabilities, since the movement of particles, which obey the laws governing the ordinary diffusion process, is described by a diffusion equation without a drift term. On the other hand, for active diffusion we used a double-peaked symmetric distribution of transition probabilities, since particles which move actively must do so with a mean walking distance in the upward (to smaller x) or downward (to larger x) direction during the unit interval of time. Therefore, we have carried out simulations with or without active diffusion, in order to ascertain whether active diffusion is detectable in the schlieren patterns.

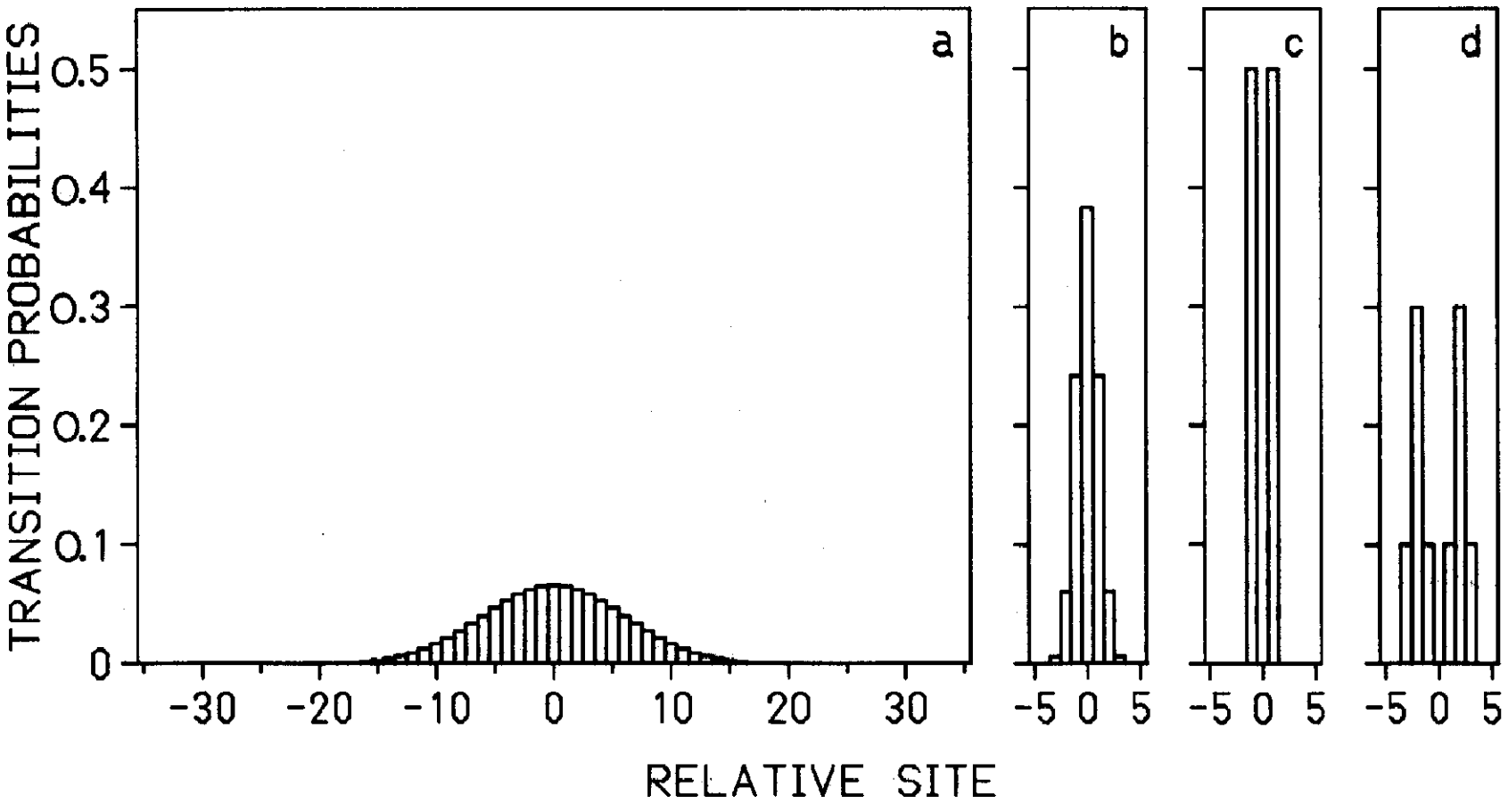

Fig. 5. Typical examples of distributions of transition probabilities for ATP (a) and MS complex (b–d). (a,b) Passive diffusion, (c) active diffusion with $D_{\text{MS active}}$ ($= D_{\text{MS passive}}$), (d) active diffusion with $D_{\text{MS active}}$ ($= 4.4 D_{\text{MS passive}}$).

Next, we investigated whether complete consumption of ATP is necessary for the hyper-sharp phenomenon. For this purpose, we introduced an ATP-regenerating system into the simulations. The method of simulating ATP regeneration on a computer is as follows: molecules of ADP hydrolyzed by myosin are converted to ATP at a slow rate in the presence of sufficient substrate as the phosphate source and a small amount of enzyme.

The results obtained in the above cases are summarized in section 3.3.

3.3. Results of simulations

We carried out simulations based on the above model with computers (Hitac M-280H and M-680H) at the Computer Centre, University of Tokyo. Typical results are shown in figs. 6–8.

Figs. 6 and 7 show concentration gradient and concentration distributions of total myosin molecules without active diffusion of myosin, respectively. It can be observed that a hyper-sharp peak appears suddenly followed by gradual growth (fig. 6) and that the hyper-sharp peak of the concentration gradient distribution corresponds to a steep

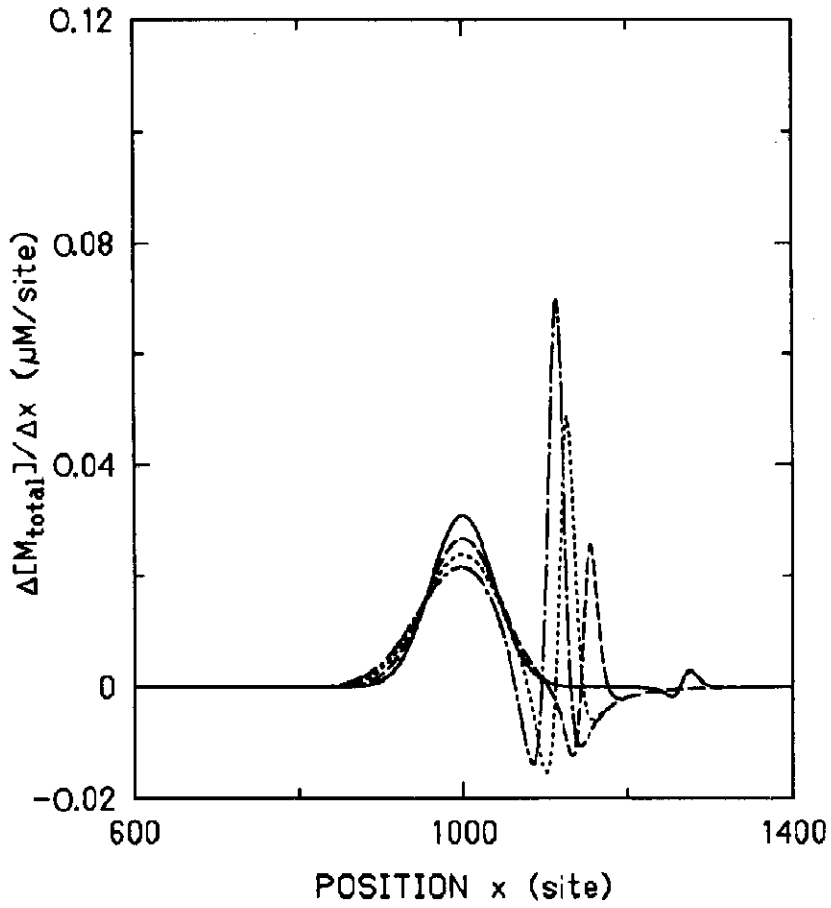

Fig. 6. Concentration gradient distributions of total myosin without active diffusion. Equilibrium constant $K = 10$. Rate constant $k_2 = 0.02\ \mu M^{-1}\ s^{-1}$. $t = 1500$ (———), 2000 (- - - - -), 2500 (· · · · · ·) and 3000 (–·–·–).

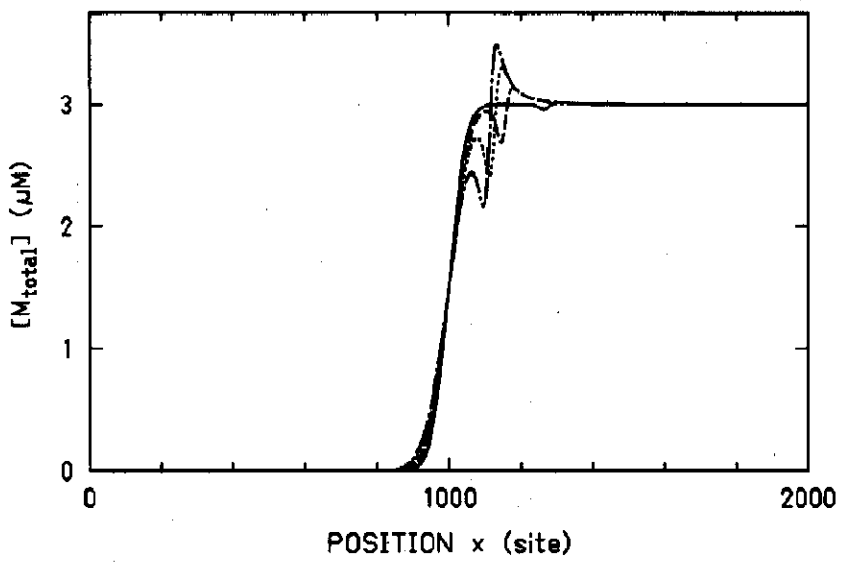

Fig. 7. Concentration distributions of total myosin without active diffusion. K and k_2 as in fig. 6. $t = 1500$ (———), 2000 (- - - - - -), 2500 (· · · · · ·) and 3000 (—·—·—).

cliff in the concentration distribution (figs. 6 and 7). Since ATP is consumed by actomyosin in the lower part of the diffusion cell, the ATP concentration in the lower part decreases gradually (fig. 8). When the ATP concentration in the lower part approaches zero, a hyper-sharp peak appears in the marginal region between the ATP-containing region and the ATP-deficient region (figs. 6 and 8).

In fig. 6, a hyper-sharp peak appears at about $t = 1500$ (the time at which the peak height becomes larger than 0.0001 μM/site, defined as the onset time of the phenomenon, is $t = 1420$). As time progresses, the peak becomes taller and moves upward (to smaller x), the movement of the peak becoming slower.

As shown in fig. 8, the ATP concentration in the lower part of the diffusion cell reached zero a little before $t = 1500$. ATP molecules in the upper part still diffuse to the lower part, but the ATP concentration in the former cannot increase, since ATP is immediately consumed by actomyosin. The ATP-deficient region expands gradually, so that the boundary of the region moves upward. This movement coincides with that of the hyper-sharp peak.

The features of the simulation results shown in figs. 6–8, such as the shapes of the schlieren patterns, behaviour of the hyper-sharp peak and change in ATP concentration with respect to onset time of the hyper-sharp peak, are in good agreement with those of the experimental results depicted in figs. 1–4. Therefore, it has been demonstrated that the second possibility for explaining the molecular mechanism mentioned in section 2 is applicable for the hyper-sharp phenomenon.

Fig. 9 shows the concentration distributions of $[M_{total}]$, $[MS_{total}]$ and $[MS_{hyd}]$ (MS_{hyd} denotes the proportion of MS being converted into AM over this unit interval of time owing to the process of hydrolysis). At $t = 1000$, almost all myosin is in the MS state. At $t = 2000$ and 3000, ATP has been consumed in the lower part of the cell and almost

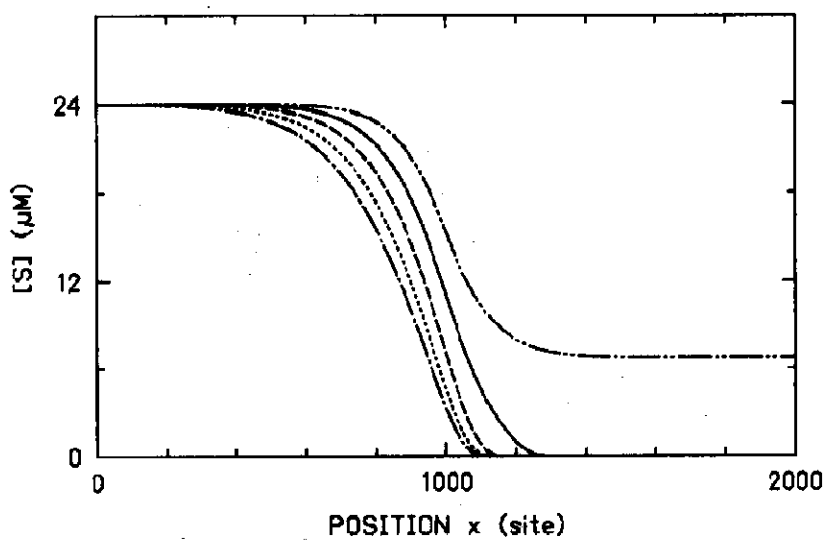

Fig. 8. Concentration distributions of free ATP without active diffusion. K and k_2 as in fig. 6. $t = 1000$ (·· — ·· — ··), 1500 (———), 2000 (- - - - - -), 2500 (· · · · · ·) and 3000 (—·—·—).

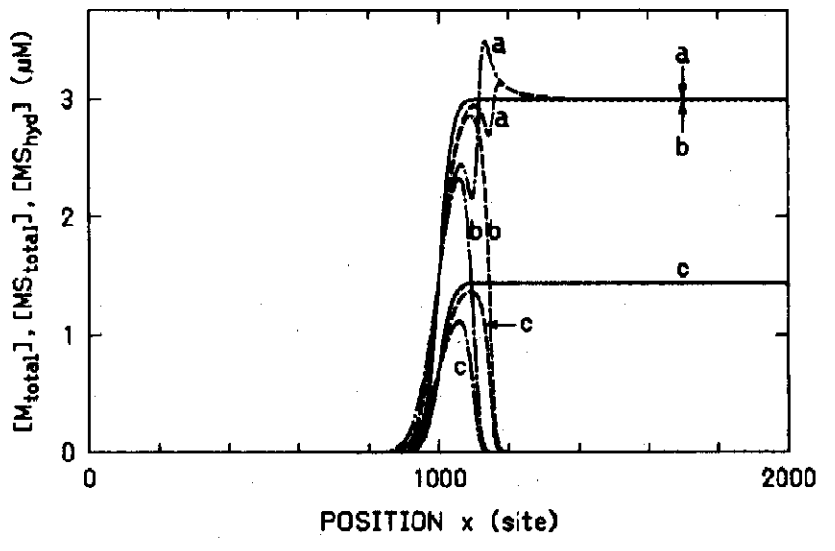

Fig. 9. Concentration distributions of various myosin species without active diffusion. K and k_2 as in fig. 6. $t = 1000$ (———, a, c; · · · · · ·, b), 2000 (- - - - - -) and 3000 (—·—·—). (a) M_{total}, (b) MS_{total}, (c) MS_{hyd} (MS_{hyd}: the part of MS becoming converted to AM over this unit interval of time owing to the process of hydrolysis).

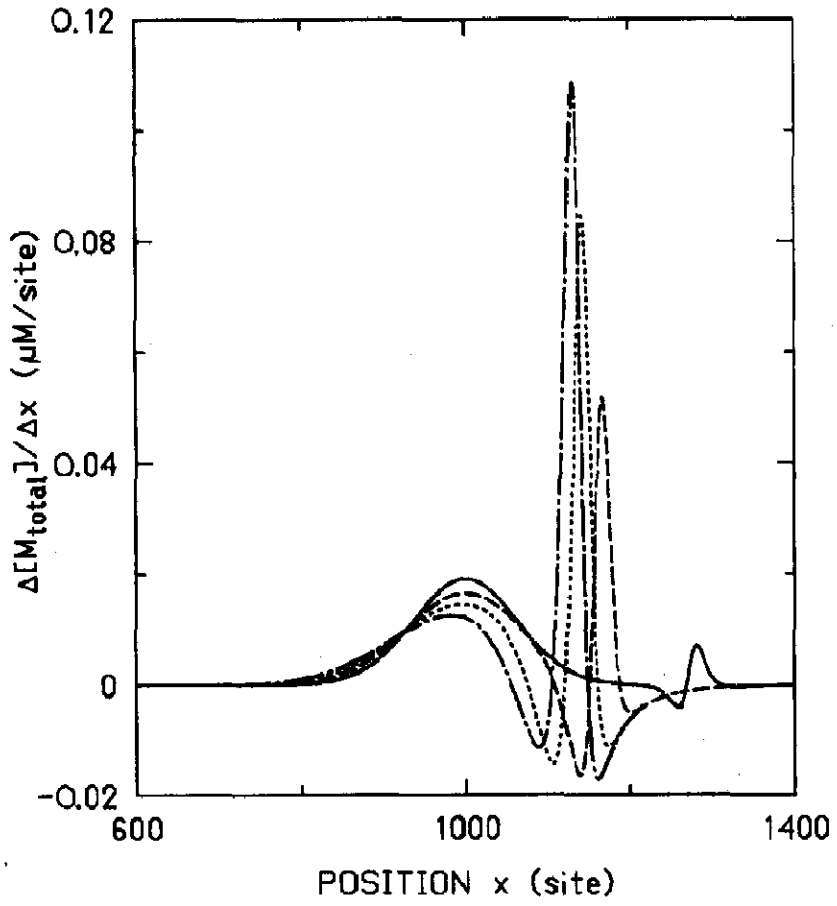

Fig. 10. Concentration gradient distributions of total myosin with active diffusion. K and k_2 as in fig. 6. $D_{\text{MS active}} = 4.4 D_{\text{MS passive}}$. $t = 1500$ (———), 2000 (- - - - - -), 2500 (· · · · · ·) and 3000 (· – · – ·).

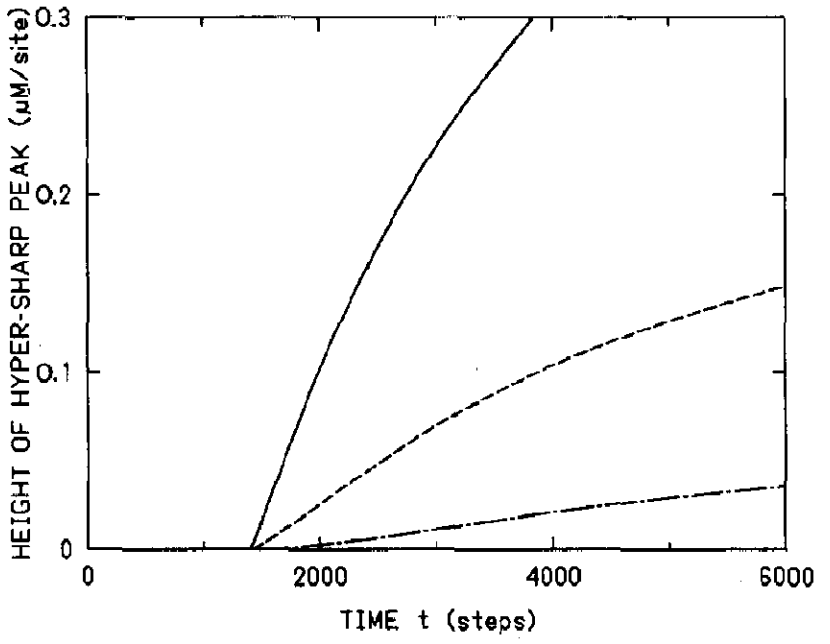

Fig. 11. Time course of change in height of hyper-sharp peak with respect to equilibrium constant. Equilibrium constant $K = 100$ (———), 10 (- - - - - -) and 1.1 (· – · – ·). Rate constant $k_2 = 0.02\ \mu M^{-1}\ s^{-1}$.

all myosin is in the AM state there. Near the boundary between the upper and lower parts of the diffusion cell, almost all myosin is still in the MS state, since sufficient ATP exists in that region. The amount of MS_{hyd} is about half of the total myosin in this case.

We carried out simulations with and without active diffusion of myosin molecules. For active diffusion, it is assumed that MS_{hyd} molecules diffuse actively while other MS molecules diffuse passively. On the other hand, in the absence of active diffusion, it is assumed that all types of MS molecules diffuse passively. For the case in which the diffusion coefficient of actively diffusing MS_{hyd}, $D_{\text{MS active}}$, is the same as $D_{\text{MS passive}}$, the diffusion patterns are exactly the same as those without active diffusion (Fig. 6), although the distribution of transition probabilities for active diffusion differs from that of passive diffusion.

In Fig. 10, the simulation condition is that the coefficient of active diffusion is 4.4-times that of passive diffusion. In this case, the main peak of the concentration gradient distribution expands more rapidly than in the case without active diffusion.

To elucidate the details of the mechanism, we have performed many further simulations with changing of the various parameters. We now summarize the results.

The growth rate of the height of the hyper-sharp peak depends on k_2, K and D_{ATP}. As demonstrated by fig. 11, the larger the value of K, the faster the growth of the hyper-sharp peak. As can be seen in fig. 12, a smaller k_2 value leads to a later onset time and slower growth of the hyper-sharp peak. The features mentioned above are evident in the experimental curves of fig. 3. The onset time of the hyper-sharp peak depends significantly on k_2, but only slightly on K.

Fig. 13 shows the reciprocal relation between the onset time and k_2. This implies that k_2 is the rate-limiting factor in ATP hydrolysis and that the hyper-sharp peak appears when all ATP in the lower part of the cell has almost been consumed.

Since it is believed that the development with respect to time of the hyper-sharp peak depends on the diffusion coefficient of ATP, we carried out simulations, varying D_{ATP} relative to the real D_{MS}. Fig. 14 demonstrates that the faster the ATP molecules diffuse, the slower the hyper-sharp peak grows. This means that myosin molecules cannot accumulate easily on actin filaments if ATP mole-

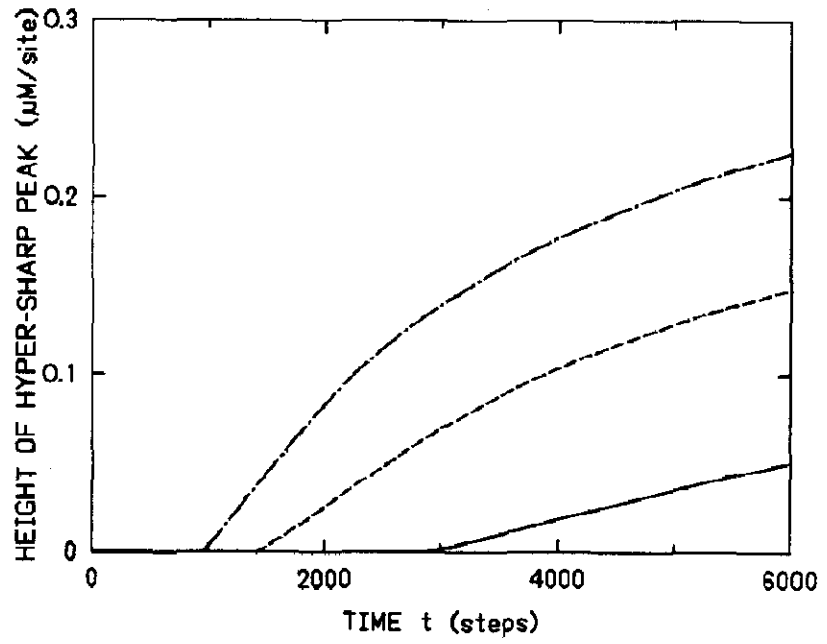

Fig. 12. Time course of change in height of hyper-sharp peak with respect to rate constant. Rate constant $k_2 = 0.01$ (———), 0.02 (- - - - - -), and 0.03 (—·—·—) $\mu M^{-1}\ s^{-1}$. Equilibrium constant $K = 10$.

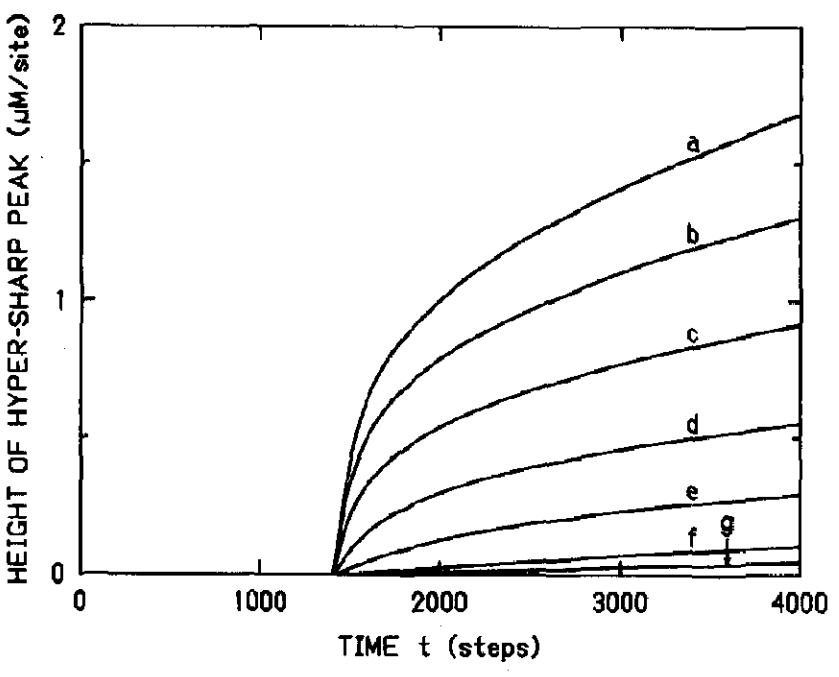

Fig. 14. Time course of change in height of hyper-sharp peak with respect to diffusion coefficient of ATP. K and k_2 as in fig. 6. $D_{ATP}/D_{MS\ passive} = 1/9$ (a), 1/3 (b), 1 (c), 3 (d), 9 (e), 36.5 (f, real ratio) and 81 (g).

cules move rapidly to the boundary region from the upper part by diffusion. In other words, the slower the ATP molecules diffuse, the more rapidly the peak grows, although the growth rate of the peak tends to saturate. In the case of ATP molecules diffusing slowly, the boundary between the ATP-containing and ATP-deficient regions should become more distinct. Hence, we can suppose that the establishment of a particular level of sharp distinction is necessary for the hyper-sharp phenomenon to occur.

The time course of the change in peak position also depends on k_2, K and D_{ATP}. As shown in fig. 15, the hyper-sharp peak appears suddenly, and moves rapidly upward (to smaller x), the move-

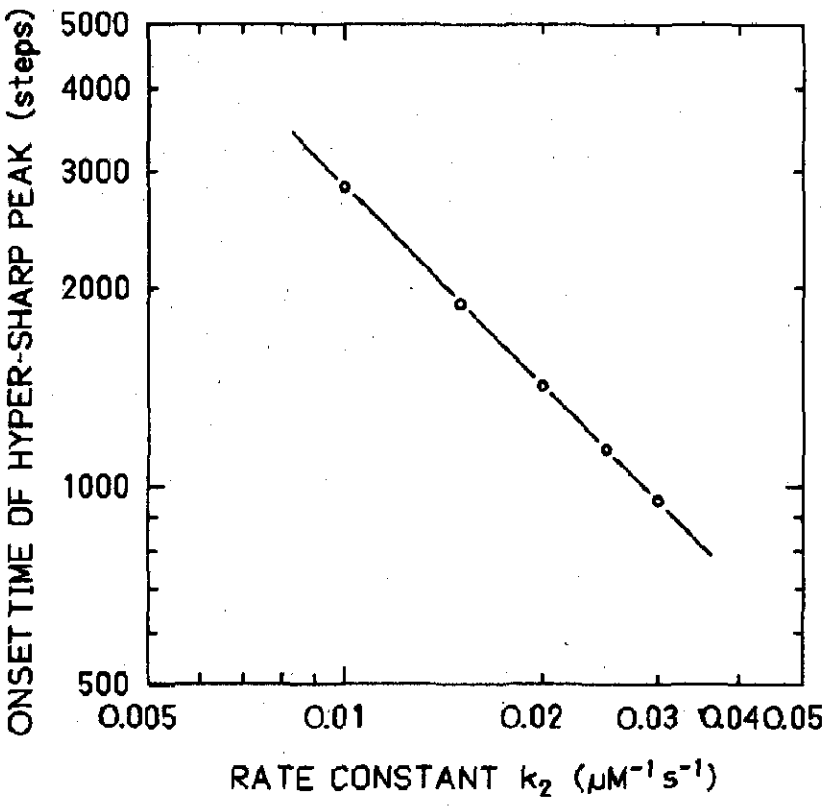

Fig. 13. Log-log plots of onset time of the hyper-sharp peak vs. rate constant k_2. Equilibrium constant $K = 10$. The onset time is defined as the time when the height of the hyper-sharp peak becomes larger than 0.0001 μM/site.

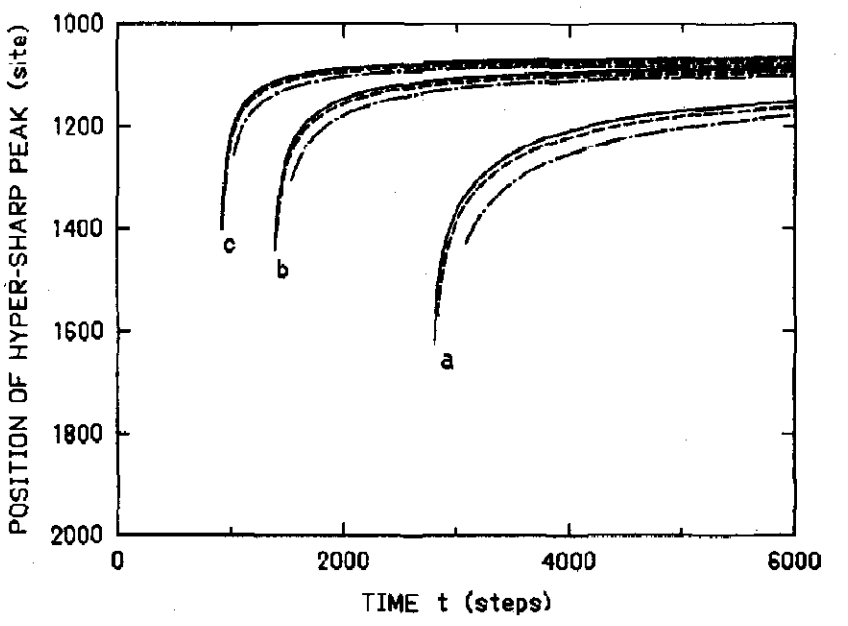

Fig. 15. Time course of change in position of hyper-sharp peak with respect to equilibrium constant and rate constant. Equilibrium constant $K = 100$ (———), 10 (- - - - - -) and 1.1 (—·—·—). Rate constant $k_2 = 0.01$ (a), 0.02 (b) and 0.03 (c) $\mu M^{-1}\ s^{-1}$. The starting point of each line indicates the onset time of the hyper-sharp peak.

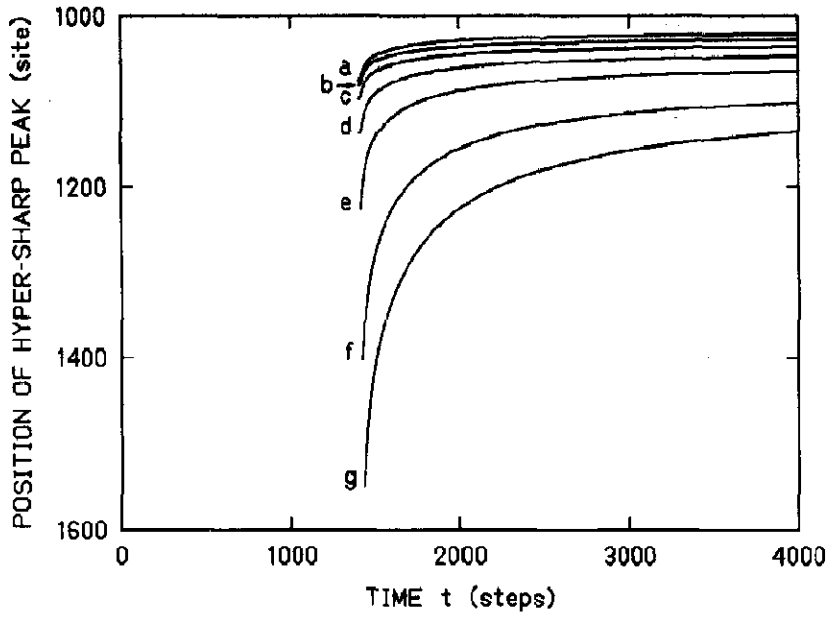

Fig. 16. Time course of change in position of hyper-sharp peak with respect to diffusion coefficient of ATP. K and k_2 as in fig. 6. $D_{ATP}/D_{MS\ passive} = 1/9$ (a), 1/3 (b), 1 (c), 3 (d), 9 (e), 36.5 (f, real ratio) and 81 (g). The starting point of each line indicates the onset time of the hyper-sharp peak.

ment then becoming slower and slower. The smaller the value of k_2, the later the peak appears, and the lower is the position of the peak. This is reasonable in view of the fact that if myosin diffuses more widely, the boundary region is formed at a lower position. The features described above can be confirmed, by inspecting the experimental curves in fig. 4. The dependence on K is less significant than that on k_2.

Fig. 16 depicts the dependence of the time course of change in peak position on the diffusion coefficient of ATP. As the diffusion of ATP becomes slower, the time course of change in peak position tends to approach a limiting curve. As stated above, the peak position coincides with the boundary of the ATP-deficient region. The boundary position should depend on the distribution of myosin, rate of ATP hydrolysis and diffusion of ATP. Therefore, it can be considered that the shapes of these lines are determined by the balance between the supply of ATP from the upper part by diffusion and the consumption of ATP by hydrolysis.

We also simulated the hyper-sharp phenomenon with the ATP-regenerating system mentioned in section 3.2. For example, even though about 70% of the myosin molecules in the lower part of the diffusion cell remain in the state of the MS complex in the presence of a small amount of ATP, the hyper-sharp peak does appear (data not shown). Therefore, it is concluded that complete consumption of ATP and permanent accumulation of myosin in the lower part of the cell are not necessary for the occurrence of the hyper-sharp phenomenon, and hence it is believed that only an imbalance in the amounts between upward and downward migration is necessary.

4. Discussion

Using the model presented in section 3, we showed that the hyper-sharp phenomenon can be simulated on a computer. All the simulation results confirm that the hyper-sharp peak can arise as a consequence of the migration of myosin molecules and their detachment/attachment from/to actin filaments, accompanied by ATP hydrolysis. If myosin molecules slide actively on actin filaments and $D_{MS\ active} \neq D_{MS\ passive}$, it would be expected that the diffusion coefficient for myosin in the presence of actin filaments would differ from that in their absence. Furthermore, as the distribution of transition probabilities for active diffusion of MS differs from that for passive diffusion, even when $D_{MS\ active} = D_{MS\ passive}$, it is expected that some difference should appear in the hyper-sharp peaks. Our computer simulations, however, show that the apparent diffusion coefficients of myosin molecules determine the shapes, sizes and development with respect to time of not only the main peak but also the hyper-sharp peak provided that D_{ATP} and k_2 remain unchanged. Moreover, they also show that the main peak of the schlieren pattern with active diffusion differs from that without its occurrence when $D_{MS\ active} \neq D_{MS\ passive}$. On the other hand, the hyper-sharp peaks show a less significant difference than the main peaks.

We were unable to detect any significant difference between the diffusion coefficients of myosin molecules in the absence and presence of actin filaments in almost all the experiments using a diffusion cell. This leads to the following hypotheses: (1) $D_{MS\ active} = D_{MS\ passive}$, or (2) MS complexes ($MS_{hyd}$) do not slide actively on actin

filaments but diffuse freely under our experimental conditions. It is difficult to determine which alternative is valid from our simulations.

The results of simulations with an ATP-regenerating system also gave good agreement with the experimental results. Namely, our simulations show that even though the ATP concentration in the lower part of the diffusion cell does not reach zero (due to slow ATP regeneration), the hyper-sharp peak appears when the concentration of ATP there becomes sufficiently low, and that of MS complexes there becomes sufficiently lower than that near the boundary. Near the boundary region between the ATP-containing and ATP-deficient regions where the hyper-sharp peak appears, downward flow of M_{total} occurs locally while only slow upward flow exists globally until the hyper-sharp peak appears. Therefore, we conclude that the hyper-sharp phenomenon is caused by singular local downward flow of myosin molecules.

Appendix: The relation between transition probabilities and the diffusion coefficient

Here, we derive a partial differential equation from a difference equation for one-dimensional random walks by using the Taylor expansion. Neglecting higher powers of the expanded series, we can obtain a diffusion-type equation. Hence, we can derive a relation between the transition probabilities and diffusion coefficient.

We now consider a one-dimensional random walk expressed as the following difference equation,

$$P(x,t) = \sum_{j=1}^{k} p_j P(x-j,t-1) + rP(x,t-1) + \sum_{j=1}^{k} q_j P(x+j,t-1) \qquad \text{(A1)}$$

where $P(x,t)$ denotes the probability that a walker is found at a site x after t time walks, p_j the transition probability from site $x-j$ to site x, q_j the transition probability from site $x+j$ to site x, and r the probability of remaining at site x. The transition probabilities are normalized, namely, $\Sigma_j(p_j+q_j)+r=1$. To derive a partial differential equation from eq. A1, we introduce continuous variables X and T related to the discrete variables x and t through the lattice distance Δx and the unit interval of time Δt. The relations are written as

$$x = \frac{X}{\Delta x}, \quad t = \frac{T}{\Delta t} \qquad \text{(A2)}$$

To define a function $\phi(X,T)$ as $\phi(X,T) = P(X/\Delta x, T/\Delta t)$, we rewrite eq. A1 as

$$\phi(X,T) = \sum_{j=1}^{k} p_j \phi(X-j\Delta x, T-\Delta t) + r\phi(X,T-\Delta t) + \sum_{j=1}^{k} q_j \phi(X+j\Delta x, T-\Delta t) \qquad \text{(A3)}$$

Taylor expansion with respect to $j\Delta x$ and Δt leads to partial differential equations. The results are as follows:

$$\sum_{i=1}^{\infty} \frac{1}{i!}(\Delta t)^i \frac{\partial^i}{\partial T^i}\phi(X,T) = \sum_{i=1}^{\infty}\sum_{j=1}^{k}\left[(-1)^i p_j + q_j\right]\frac{1}{i!}(j\Delta x)^i \times \frac{\partial^i}{\partial X^i}\phi(X,T) \qquad \text{(A4)}$$

$$\sum_{i=1}^{\infty} \frac{1}{(2i)!}(\Delta t)^{2i} \frac{\partial^{2i}}{\partial T^{2i}}\phi(X,T) = -\frac{1}{2}\sum_{i=2}^{\infty}\frac{1}{i!}\sum_{l=1}^{i-1}\sum_{j=1}^{k}\left[(-1)^i p_j + (-1)^{i-l} q_j\right] \times {}_iC_l (j\Delta x)^l (\Delta t)^{i-l} \frac{\partial^l}{\partial X^l}\frac{\partial^{i-l}}{\partial T^{i-l}}\phi(X,T) \qquad \text{(A5)}$$

The former result (eq. A4) is obtained from eq. A1 under the condition of invariance with respect to time of eq. A1. The latter result (eq. A5) represents the restriction reduced by the condition of small time (Δt) invariance of eq. A3. We obtain the diffusion-type equation from eq. A4 taking

only first-order terms of Δt into account, namely,

$$\frac{\partial}{\partial T}\phi(X,T)=\sum_{i=1}^{\infty}\sum_{j=1}^{k}\left[(-1)^i p_j+q_j\right]\frac{1}{i!}\times j^i\frac{(\Delta x)^i}{\Delta t}\frac{\partial^i}{\partial X^i}\phi(X,T) \qquad \text{(A6)}$$

Moreover, we also obtain eq. A6 from eq. A5 taking second-order terms of Δt into account as far as $\Delta t \to 0$.

Taking terms of Δx up to those of the second order, one can obtain from eq. A6 the so-called Fokker-Planck equation. The Fokker-Planck equation derived from eq. A6 becomes

$$\frac{\partial\phi(X,T)}{\partial T}=-\sum_{j=1}^{k}(p_j-q_j)j\frac{\Delta x}{\Delta t}\frac{\partial}{\partial X}\phi(X,T)+\frac{1}{2}\sum_{j=1}^{k}[p_j+q_j]j^2\frac{(\Delta x)^2}{\Delta t}\times\frac{\partial^2}{\partial X^2}\phi(X,T) \qquad \text{(A7)}$$

Since in the case $p_j=q_j$ eq. A7 yields a so-called diffusion equation, we can express in a straightforward manner the relation between a diffusion coefficient D and transition probabilities p_j and q_j, i.e.,

$$D=\frac{1}{2}\sum_{j=1}[p_j+q_j]j^2\frac{(\Delta x)^2}{\Delta t} \qquad \text{(A8)}$$

References

1 H. Asai, J. Phys. Soc. Jap. 36 (1974) 1114.
2 H. Kagawa and H. Asai, Bull. Sci. Eng. Lab. Waseda Univ. 84 (1979) 50 (in Japanese).
3 H. Kagawa and H. Asai, J. Biol. Chem. 255 (1980) 7106.
4 H. Kagawa and H. Asai, J. Biochem. (Tokyo) 84 (1978) 957.
5 W. Feller, An introduction to probability theory and its applications, vol. 1, 3rd edn. (Wiley, New York, 1968).
6 H. Neurath, Science 93 (1941) 431.
7 R. Josephs and W.F. Harrington, Proc. Natl. Acad. Sci. U.S.A. 58 (1967) 1587.